JOURNAL OF BACTERIOLOGY, Jan. 1973, p. 387-393

Vol. 113, No. 1
Printed in U.S.A.

Ultrastructure of Free-Living and Nitrogen-Fixing Forms of *Rhizobium meliloti* as Revealed by Freeze-Etching

C. R. MACKENZIE, W. J. VAIL, AND D. C. JORDAN

Department of Microbiology, College of Biological Science, University of Guelph, Guelph, Ontario, Canada

Received for publication 27 September 1972

Freeze-etching of *Rhizobium meliloti* provided considerable insight into the ultrastructure of this bacterium and into the changes accompanying the transformation from the free-living rod forms to the nitrogen-fixing bacteroid forms. In the small rods, one cleavage plane was revealed at the level of the cell wall and a second at the level of the plasma membrane. Very little structure was evident at the cell wall level, but distinctly different convex and concave fracture faces were exposed at the cell membrane cleavage plane. During the transformation into the bacteroidal state the wall decreased in thickness, became less rigid, and developed a particulate surface. In addition, changes in particle density were observed in the plasma membrane. The fine structure of the plant membranes, the infection threads, and the arrangement of the bacteroids within the plant cells also were revealed.

The ultrastructure of legume root nodules has been studied by several workers, and considerable insight has been gained into the nature of the effective nitrogen-fixing symbiosis between the root nodule bacteria and the host plant (3, 5, 7, 10, 12, 13). The free-living forms of the bacteria enter the plant roots through the root hairs and migrate in an infection thread towards the cortical cells. These infection threads enter the cortical cells releasing the bacteria. At this stage the small rod forms of the bacteria are transformed into the enlarged and distorted bacteroids and become, in effect, nitrogen-fixing organelles of the plant cells. The changes undergone by the bacteria during this transformation remain somewhat unclear. At the time of entry into the plant cells or shortly thereafter, the bacteria become surrounded by a plant-produced enclosing membrane; the origin of this membrane has been the subject of considerable controversy. We have employed the freeze-etch technique in an attempt to elucidate some of these phenomena.

MATERIALS AND METHODS

Culture and growth conditions. The organism used was *Rhizobium meliloti* strain R21, an organism which forms an effective nitrogen-fixing symbiosis with alfalfa. Cells were grown to mid-log phase in a medium containing 0.5 g of K_2HPO_4, 0.2 g of $MgSO_4 \cdot 7H_2O$, 0.1 g of NaCl, and 3 g of Difco yeast extract per liter of distilled water.

Growth of plants. Seeds of alfalfa (*Medicago sativa*), variety Iroquois, were surface-sterilized and planted in sterile sand containing a nitrogen-free nutrient solution. The seedlings were inoculated with *R. meliloti* R21 10 days after planting. The root nodules were picked 2 weeks after inoculation.

Electron microscopy. For freeze-etching or freeze-fracturing, the bacterial cells and root nodules were placed in 30% dimethylsulfoxide (DMSO) or 30% glycerol overnight at room temperature. The samples were frozen in Freon-22, placed in liquid nitrogen, and fractured at -100 C at 2×10^{-6} torr with a Balzer BA360 freeze-etch unit. The replicas were prepared by the method of Vail and Riley (17).

RESULTS

Figure 1 shows a longitudinal section of an infection thread as seen in the freeze fracture. It is difficult to see the structure of the bacteria in infection threads in thin section because they are surrounded by slimy material which results in poor fixation. However, this problem is eliminated by using the freeze-fracture technique, and the invading bacteria seem to be very similar to the small rods grown in culture (see Fig. 4). Inclusion bodies, which are generally assumed to be polyhydroxybutyric acid (5, 10), could be seen in the cells.

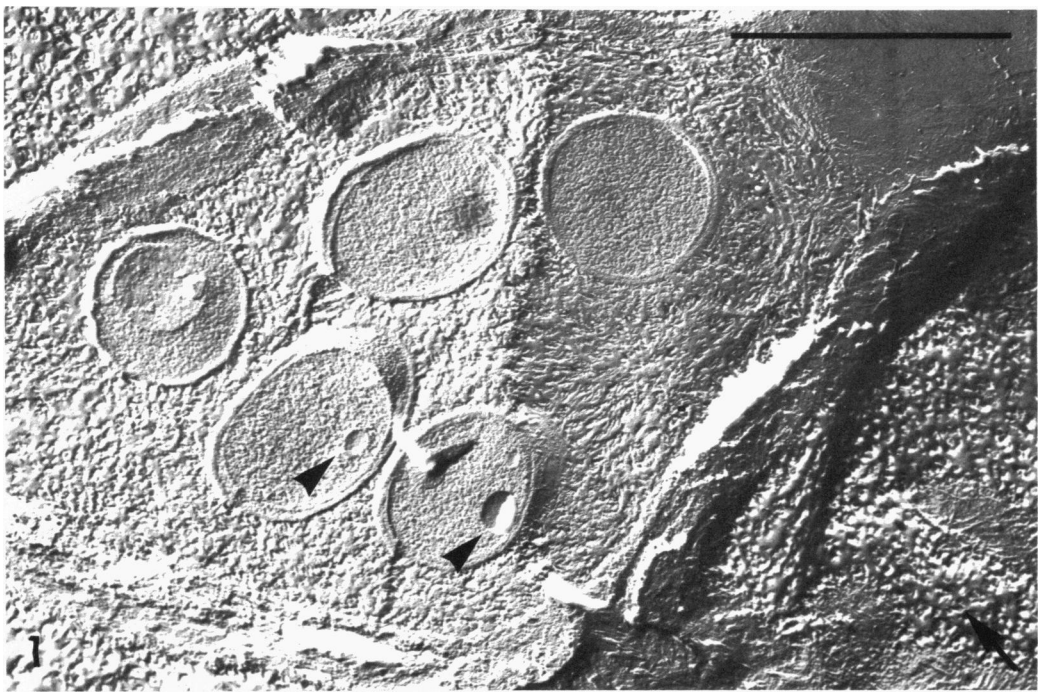

FIG. 1. *Freeze-fracture replica of an infection thread. Arrows show polyhydroxybutyric acid granules. Arrow in lower right indicates direction of shadow. Bar represents 1 μm in Fig. 1 through 3.*

At low magnifications, freeze-etch replicas show the arrangement of the bacteroids in the plant cells in excellent three-dimensional detail (Fig. 2). DMSO was found to give better results when low-magnification views were desired. However, glycerol was found to provide a better suspending medium for examining the ultrastructure of the various membranes at higher magnifications. At higher magnifications the detail of the complex membrane systems becomes more evident. Figure 3 shows fracture planes at the levels of the bacteroid cell wall and the enclosing membrane surrounding the bacteroids.

When the small rod forms from fluid culture are examined, the situation is less complicated and quite different (Fig. 4). Two distinct fracture faces are exposed in the plasma membrane. If the membrane splits, as is generally assumed (4, 16), the convex fracture face represents the outer surface of the inner half of the membrane and the concave face represents the inner surface of the outer half of the membrane. The convex surface is very particulate, whereas the particles are sparse on the concave surface. One of the cells in this figure is cross-fractured. It is interesting to note that these cells are congregating around some unidentified bodies thereby forming a rosette, an arrangement commonly seen by light microscopy. The bacteroid plasma membrane (Fig. 5) is distinctly different from that of the small rods. The particles are smaller and do not completely cover the convex fracture face; nonparticulate areas are often seen.

The cell walls of the small rods and bacteroidal forms also showed differences. The surface revealed by fracturing the small rods is rather rough but nonparticulate (Fig. 6). The bacteroid wall, on the other hand, is sparsely covered with particles (Fig. 3, 9). There is the possibility that this is contamination originating from material in the space between the wall and the enclosing membrane, but this seems unlikely since the particle density is quite consistent. There is also an obvious difference in cell wall thickness between the two forms. In the small rods the thickness of the wall is almost double that of the plasma membrane (Fig. 7), but these two structures are of approximately the same thickness in the bacterioids (Fig. 8). In Fig. 7 particles can be seen lined up in the plasma membrane, whereas the wall appears rather structureless. The bacteroid walls appear to be much less rigid than those of the small rods. In Fig. 5 pieces of wall are seen to be torn away from the membrane; this is contrast to the small rods in which the rigid cell wall almost invariably cleaves completely away from the membrane (Fig. 4).

The surface revealed by the fracture at the

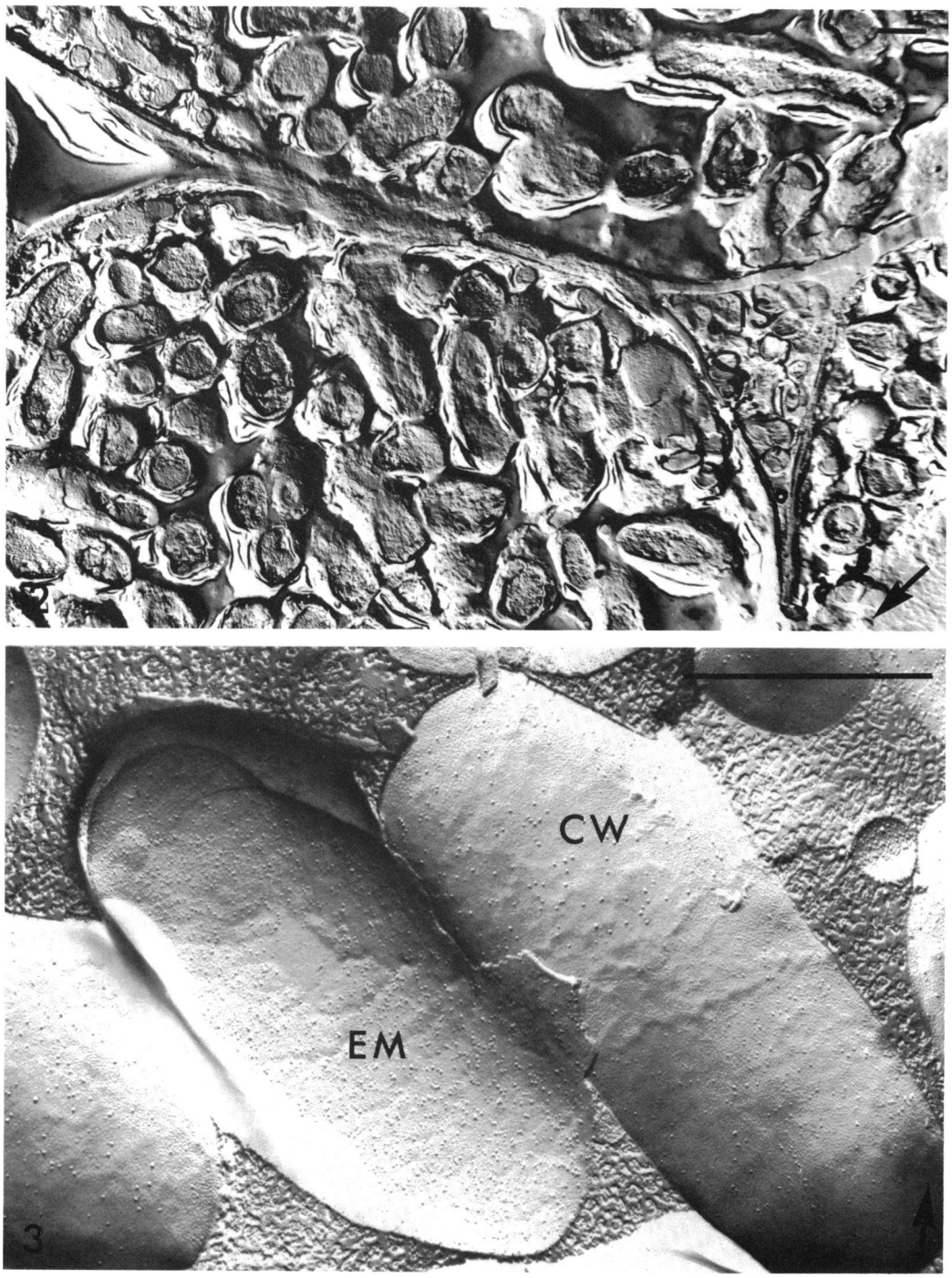

FIG. 2. *Freeze-etch replica (DMSO) showing the arrangement of the bacteroids in the plant cells. IS, intracellular space containing small rod forms of the bacteria.*

FIG. 3. *Freeze-fracture replica of several bacteroids.*

level of the enclosing membrane was very characteristic; it was a surface with particles rather sparsely and irregularly distributed (Fig. 3, 9). In Fig. 9 the membrane appears to have split, and both the surface and membrane interior are exposed. The bacteroid wall with its

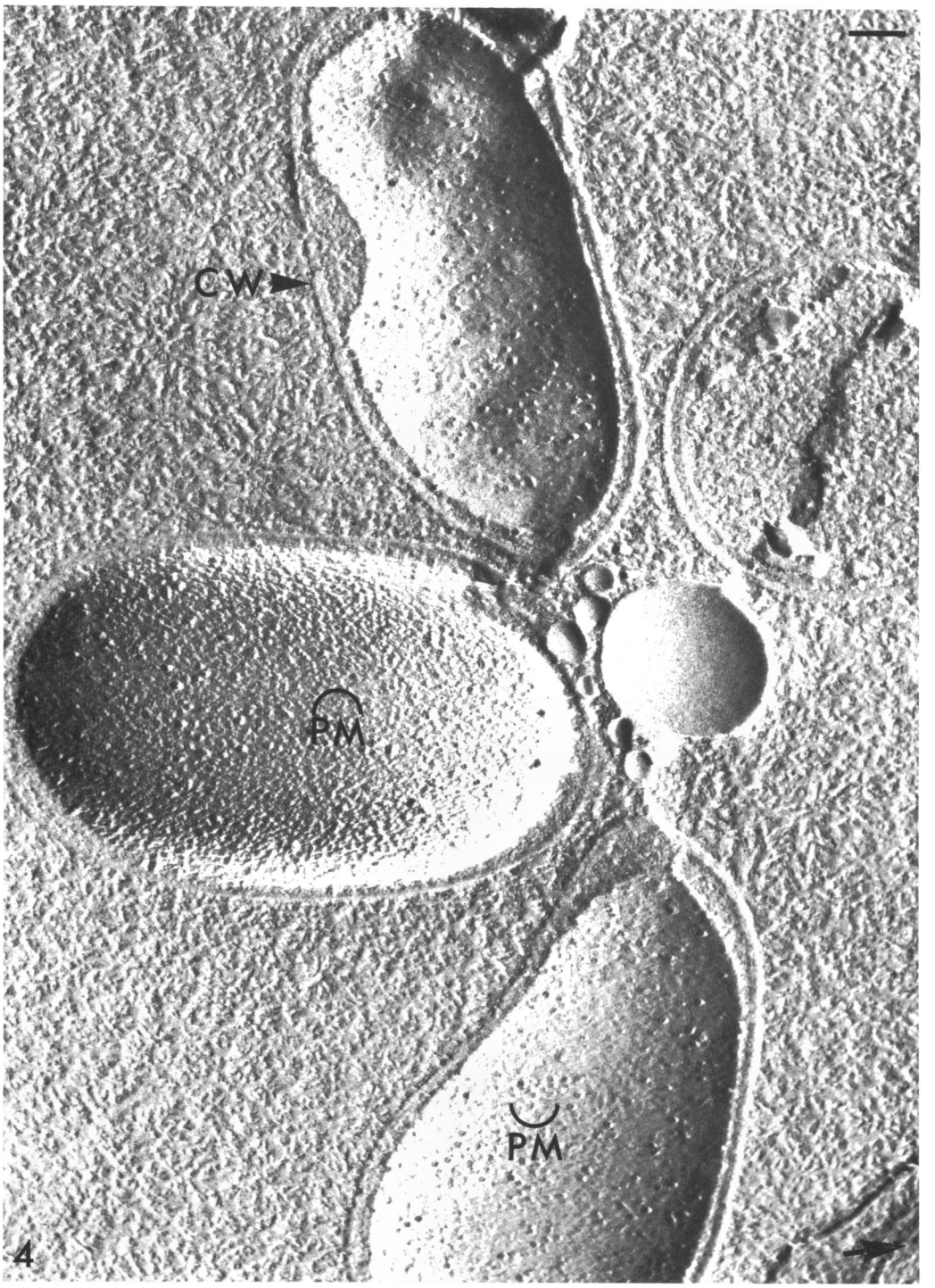

FIG. 4. *Freeze-fracture replica of small rod forms.* $\widehat{PM}$, *convex fracture face of plasma membrane;* $\overset{\smile}{PM}$, *concave fracture face of plasma membrane. Bar represents 0.1 μm in Fig. 5 through 12.*

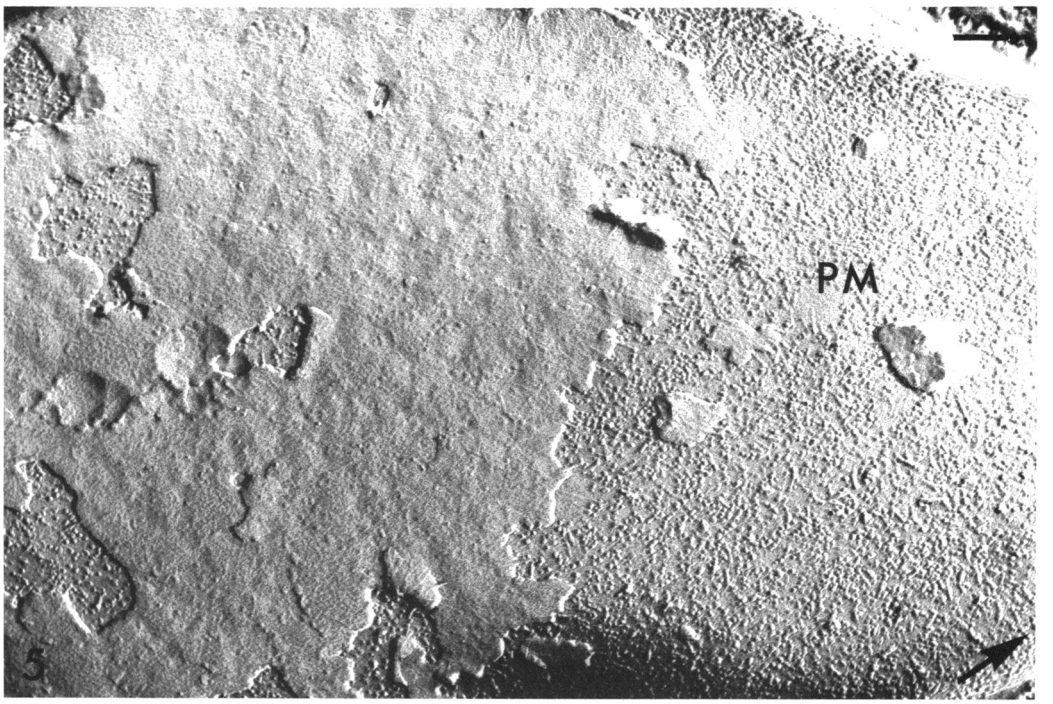

FIG. 5. *Bacteroid plasma membrane with pieces of wall attached.*

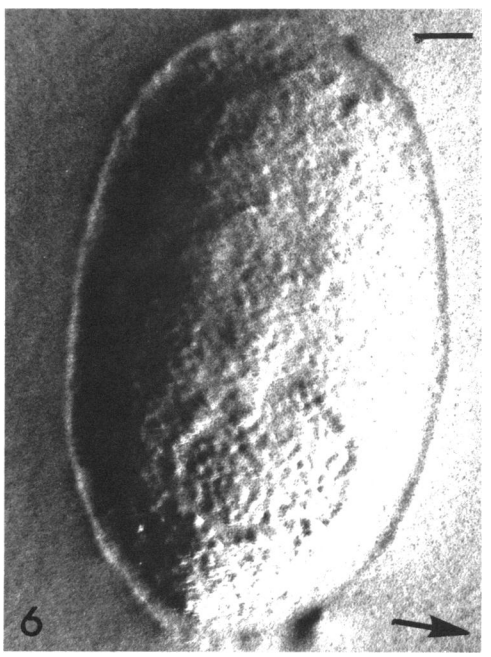

FIG. 6. *Cell wall cleavage plane of small rod form.*

characteristic fracture face is also revealed. The plant-produced enclosing membrane is quite different from what is believed to be the plasma membrane of the plant cell (Fig. 10). This membrane is believed to be the plant plasma membrane because the large sheets of this membrane observed practically eliminated any other possibility. The particles on the latter are larger and more uniform in size; the particle density is also less.

DISCUSSION

The freeze-fracture studies on the small rods agree closely with what has been reported for other gram-negative bacteria (2, 6, 9, 18). There appear to be only two major fracture planes—one through the membrane and a second at the level of the cell wall. Some workers have suggested that there are several fracture planes in the cell wall, but the evidence is weak (14, 15). The organism used here appears to be rather different from other gram-negative bacteria studied in that the cell wall has a tendency to cleave completely away from the membrane. The exposure of two distinct fracture faces in the plasma membrane also was very obvious here.

Whereas in thin section the bacteroid plasma membrane, cell wall, and enclosing membrane appear practically identical and indistinguishable from most other biological membranes, the freeze-etch technique has enabled us to show

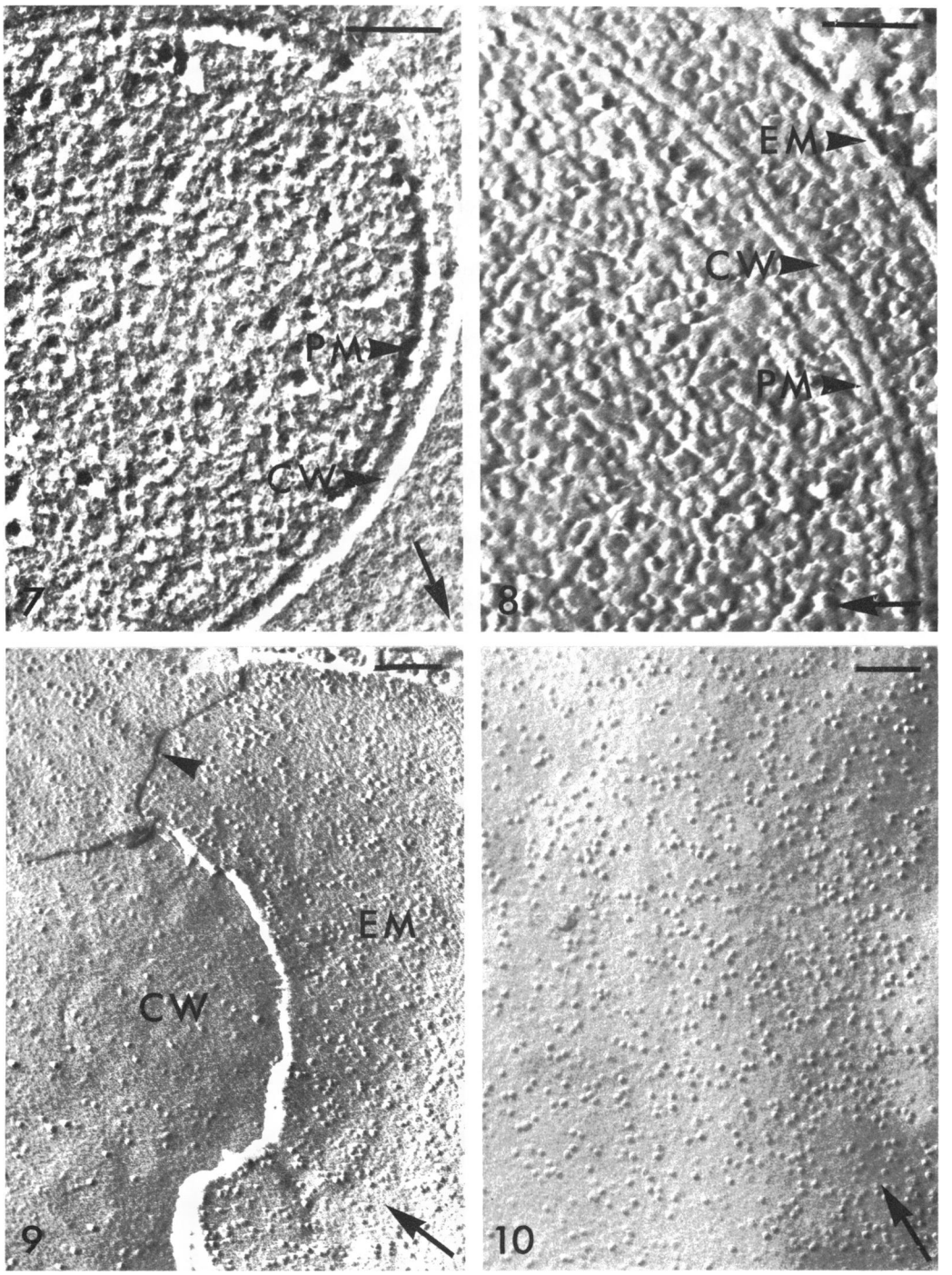

FIG. 7. *Cross-fractured small rod showing thickness of plasma membrane and cell wall.*
FIG. 8. *Cross-fractured bacteroid showing thickness of plasma membrane and cell wall.*
FIG. 9. *Enclosing membrane and bacteroid cell wall. Arrow shows splitting of enclosing membrane.*
FIG. 10. *Plant plasma membrane.*

distinct differences in the structure of these membranes and to trace the ultrastructural changes that occur in the wall and membrane during the transformation into the bacteroidal forms.

The observations made with regard to changes in wall structure are consistent with previous observations in which an inhibition of wall synthesis was found to occur (11). This inhibition would logically lead to a thinner and less rigid wall, as appears to be the case.

It appears that major changes occur in the protein composition of the plasma membrane during the conversion of the rod forms of this bacterium into the nitrogen-fixing forms. This presumably reflects a change in function and indicates that this membrane may play an important role in the fixation process. Studies on the cytochrome composition of the two forms of *R. japonicum* also have suggested that a change in membrane composition and function occurs during the conversion of small rods to bacteroids, with cytochrome *a* being found in the rods but absent in the bacteroids (1, 8).

The structure of the enclosing membrane gives some clue as to its origin. Two major hypotheses have been proposed for the formation of this enclosing membrane. One suggests that it is formed from the plant plasma membrane as the bacteria enter the cortical cells (3, 7, 10). The second hypothesizes that the membrane is formed de novo shortly after the bacteria enter the plant cells (5, 12). Though not confirming either of these hypotheses, the observation made here concerning the differences in structure between the plant plasma membrane and the enclosing membrane tends to refute the first of these two suggestions, at least for *R. meliloti*.

ACKNOWLEDGMENTS

The financial support of the National Research Council of Canada in the form of grant A-772 to D.C.J. and a postgraduate scholarship to C.R.M. is acknowledged.

LITERATURE CITED

1. Appleby, C. A., and F. J. Bergersen. 1958. Cytochromes of *Rhizobium*. Nature (London) **182**:1174.
2. Bayer, M. E., and C. C. Remsen. 1970. Structure of *Escherichia coli* after freeze-etching. J. Bacteriol. **101**:304-313.
3. Bergersen, F. J., and M. J. Briggs. 1958. Studies on the bacterial component of soybean root nodules: cytology and organization in the host tissue. J. Gen. Microbiol. **19**:482-490.
4. Branton, D. 1969. Membrane structure. Annu. Rev. Plant Physiol. **20**:209-238.
5. Dart, P. J., and F. V. Mercer. 1963. Development of the bacteroid in the root nodule of barrel medic (*Medicago tribuloides* Desr.) and subterranean clover (*Trifolium subterraneum* L.). Arch. Mikrobiol. **46**:382-401.
6. De Voe, I. W., J. W. Costerton, and R. A. MacLeod. 1971. Demonstration by freeze-etching of a single cleavage plane in the cell wall of a gram-negative bacterium. J. Bacteriol. **106**:659-671.
7. Dixon, R. O. D. 1964. The fine structure of infection threads, bacteria, and bacteroids in pea and clover nodules. Arch. Mikrobiol. **48**:166-178.
8. Falk, J. E., C. A. Appleby, and R. J. Porra. 1959. The nature, function and biosynthesis of haem compounds and porphyrins of legume root nodules. Symp. Soc. Exp. Biol. **13**:73-86.
9. Fiil, A., and D. Branton. 1969. Changes in the plasma membrane of *Escherichia coli* during magnesium starvation. J. Bacteriol **98**:1320-1327.
10. Goodchild, D. J., and F. J. Bergersen. 1966. Electron microscopy of the infection and subsequent development of soybean root nodule cells. J. Bacteriol. **92**:204-213.
11. Jordan, D. C., and W. H. Coulter. 1965. On the cytology and synthetic capacities of natural and artificially produced bacteroids of *Rhizobium leguminosarum*. Can. J. Microbiol. **11**:709-720.
12. Jordan, D. C., and I. Grinyer. 1965. Electron microscopy of the bacteroids and root nodules of *Lupinus luteus*. Can. J. Microbiol. **11**:721-725.
13. Jordan, D. C., I. Grinyer, and W. H. Coulter. 1963. Electron microscopy of infection threads and bacteria in young root nodules of *Medicago sativa*. J. Bacteriol. **86**:125-137.
14. Lickfeld, K. G., M. Achterrath, F. Hentrich, L. Kolehmainen-seveus, and A. Persson. 1972. Die Feinstrukturen von *Pseudomonas aeruginosa* in ihrer Deutung durch die Gefrieratztecknik, Ultramikrotomie und Kryo-ultramikrotomie. J. Ultrastruct. Res. **38**:27-45.
15. Nanninga, N. 1970. Ultrastructure of the cell envelope of *Escherichia coli* B after freeze-etching. J. Bacteriol. **101**:297-303.
16. Nanninga, N. 1971. Uniqueness and location of the fracture plane in the plasma membrane of *Bacillus subtilus*. J. Cell Biol. **49**:564-570.
17. Vail, W. J., and R. K. Riley. 1971. Ultrastructure of isolated heavy beef heart mitochondria revealed by the freeze-etching technique. Nature (London) **231**:525-527.
18. Van Gool, A. P., and N. Nanninga. 1971. Fracture faces in the cell envelope of *Escherichia coli*. J. Bacteriol. **108**:474-481.